

Extremely Large Group-Velocity Dispersion of Line-Defect Waveguides in Photonic Crystal Slabs

M. Notomi,¹ K. Yamada,² A. Shinya,¹ J. Takahashi,² C. Takahashi,² and I. Yokohama¹

¹NTT Basic Research Labs., NTT Corporation, 3-1 Morinosato-Wakamiya, Atsugi, 243-0198 Japan

²NTT Telecommunications Energy Labs., NTT Corporation, 3-1 Morinosato-Wakamiya, Atsugi, 243-0198 Japan

(Received 12 August 2001; published 30 November 2001)

We reveal experimentally waveguiding characteristics and group-velocity dispersion of line defects in photonic crystal slabs as a function of defect widths. The defects have waveguiding modes with two types of cutoff within the photonic band gap. Interference measurements show that they exhibit extraordinarily large group dispersion, and we found waveguiding modes whose traveling speed is 2 orders of magnitude slower than that in air. These characteristics can be tuned by controlling the defect width, and the results agree well with theoretical calculations, indicating that we can design light paths with *made-to-order* dispersion.

DOI: 10.1103/PhysRevLett.87.253902

PACS numbers: 42.70.Qs, 42.25.Bs

A periodically modulated refractive-index structure, namely photonic crystal (PC), can possess a photonic band gap (PBG) under certain conditions, thus enabling it to function as a photonic insulator [1,2]. If we introduce a line or point defect into such photonic insulators, we can build wavelength (λ) scale optical waveguides or resonators, thus making PCs possible candidates for the platforms of future photonic LSIs [3]. Line-defect waveguides (LDWGs) in PCs are receiving considerable attention because their waveguiding mechanism is fundamentally different from that of conventional dielectric waveguides, such as optical fibers, which rely on total internal reflection. This difference allows us theoretically to expect various unique properties not provided by conventional waveguides. For example, theory predicts that it is possible to realize a λ -scale sharp bend with LDWGs [4]. Another notable feature of LDWGs is their group-velocity dispersion characteristics that differ greatly from those of conventional waveguides. The dispersion of LDWGs is largely tunable by designing the line defect structures as described later. The unusual dispersion may lead to a variety of interesting optical nonlinearity phenomena such as soliton propagation or wavelength conversion, and may also be employed for dispersion management devices demanded by photonic information technology.

In this regard, a PC slab that is a $\lambda/2$ -thick high-refractive-index dielectric slab (e.g., Si) having two-dimensional (2D) periodic air holes sandwiched between air claddings is one of the most promising PC structures. It can serve as an ideal 2D photonic crystal because of the strong vertical confinement within the 2D plane. Recently, the formation of the 2D PBG in TE polarization ($\mathbf{E} \parallel$ 2D plane) for PC slabs has been confirmed by transmission measurements [5,6]. Light transmission through line defects in PC slabs have also been observed [7–9], but detailed spectroscopic measurements have been very limited and it has not been directly shown that LDWGs have dramatically different characteristics from conven-

tional waveguides, especially in terms of their dispersion. Concerning the dispersion, PC fibers have received much attention [10], but they are fundamentally different from LDWGs in PC slabs since they do not have periodicity in the propagation direction or real PBGs within the 2D plane.

In this Letter, we experimentally study the wavelength dependence of guiding modes of a series of line defects of Si photonic crystal slabs that are fabricated by semiconductor nanofabrication technology and reveal that their group-velocity dispersion characteristics are fundamentally different from those of conventional waveguides by spectroscopic measurements.

We fabricated 2D hexagonal air-hole Si PC slabs (lattice constant a is $0.39 \mu\text{m}$) with single-line defects by e -beam lithography and electron-cyclotron-resonance ion-stream plasma etching using silicon-on-insulator substrates [11]. The underlying SiO_2 layer was removed by selective wet etching using HF solution. This resulted in the air-clad 2D Si PC slabs shown in Fig. 1. Since our fabrication technology guarantees the resolution of $<5\%$ in diameter and $<1\%$ in distance between the holes, we could control the important geometrical parameters very precisely. We prepared a series of LDWG samples having various defect widths w_d and defect lengths l_d . The hole diameter is set to $0.55a$, and each line defect is connected to a $10\text{-}\mu\text{m}$ -wide Si ridge waveguide which is used as an output port. We measured the transmission spectra in the $1.2\text{--}1.7 \mu\text{m}$ range by using a set of wide-band superluminescent diodes as a light source. We directly coupled linearly polarized light to an LDWG from a polarization-maintaining single-mode tapered fiber. All the measurements were made with TE polarization.

To realize LDWGs, the PC slabs should have wide PBG within the 2D plane. Figure 2(a) shows the transmission spectrum of defect-free PC slabs in the Γ -K and Γ -M direction, which clearly proves that our samples have 2D PBG from 1.22 to $1.58 \mu\text{m}$ for TE polarization. Next, we investigated LDWGs where a single air-hole line had

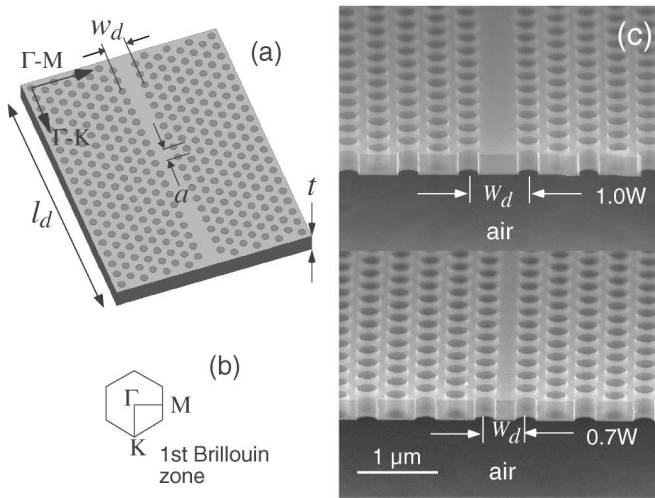


FIG. 1. Single missing-hole line defects of Si hexagonal air-hole PC slabs. The slab thickness is $0.2 \mu\text{m}$. The defect width w_d is defined as the spacing between the center of air holes nearest to defects. (a) Schematic of samples, (b) reciprocal-space representation, (c) scanning electron micrographs of fabricated samples ($w_d = 1.0$ and $0.7W$).

been removed from the hexagonal PC. Figure 2(b) shows the transmission spectrum of the LDWG with $w_d = 1.0W$ ($W = \sqrt{3}a$) and $l_d = 172 \mu\text{m}$ ($441a$). The effect of introducing defects is clearly visible in the spectrum. A single waveguiding mode appears in the PBG, which has two distinctive cutoffs. We next examined the w_d depen-

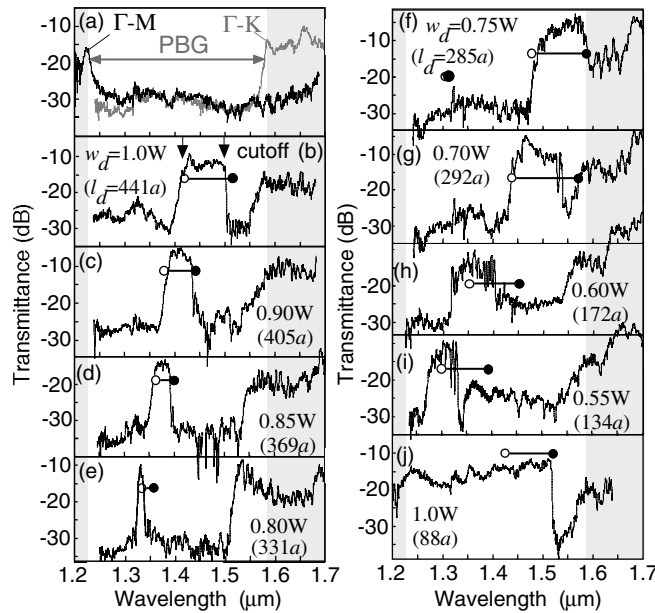


FIG. 2. Transmission spectra (TE polarization): (a) defect-free PCs, (b)–(i) line defects of various widths, (j) the same as (b) but with shorter length. Theoretically calculated transmission windows are represented by horizontal bars (solid and open circles are cutoff points due to the mode gap, and the light line). The values are normalized by the transmission of ridge waveguides with the same length.

dence. The measured spectra for various w_d are shown in Figs. 2(c)–2(i). Each LDWG has a clear waveguiding mode with cutoffs, and the width and position of the waveguiding mode depends strongly on w_d . The mode shifts to higher frequency as w_d decreases from 1.0 to 0.8 W . But a new mode appears at a lower frequency for 0.75 W , and this becomes a single waveguiding mode for $w_d < 0.75W$.

To obtain a comprehensive understanding of the underlying physics of what we observed, we calculated the theoretical dispersion curves (shown in Fig. 3) of the LDWGs by directly solving time-dependent Maxwell equations with the 3D finite-difference time-domain (FDTD) method. We hereafter use normalized frequency (a/λ) and wavevector (ka). The calculated curves are fairly complicated, but they are basically composed from two contributions that are shown by broken lines in the figure: one originates from refractive-index guiding (IG) modes (linear curves) and the other from PBG guiding (GG) modes (S -shaped curves). IG modes are similar to dielectric waveguide modes and GG modes resemble microwave metallic-wall waveguide modes. The calculated curves can be understood as a mixture of these IG and GG modes, and their folded modes. Anticrossing occurs at the intersecting points, which produces mode gaps within the PBG. The observed lower-frequency cutoff corresponds to this mode gap. Furthermore, when the mode is located inside the clad light line, it becomes leaky [12]. The estimation we obtained by the FDTD method shows that the propagation loss at a point inside the light line [shown as + in Fig. 3(a)] is 119.5 dB/mm. This finite propagation distance is the origin of higher-frequency cutoffs.

To examine directly whether this interpretation can be applied to our experiments, we plot theoretical transmission windows determined from the above interpretation in

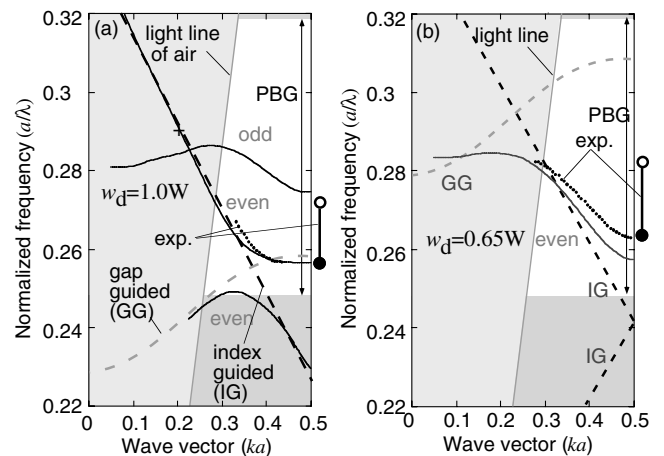


FIG. 3. Theoretical dispersion curves of line defects of PC slabs: (a) $w_d = 1.0W$ (b) $w_d = 0.65W$. Solid lines are 3D FDTD calculations. Broken lines illustrate hypothetical IG and GG modes. Solid dots are experimentally determined dispersion from the result in Fig. 4.

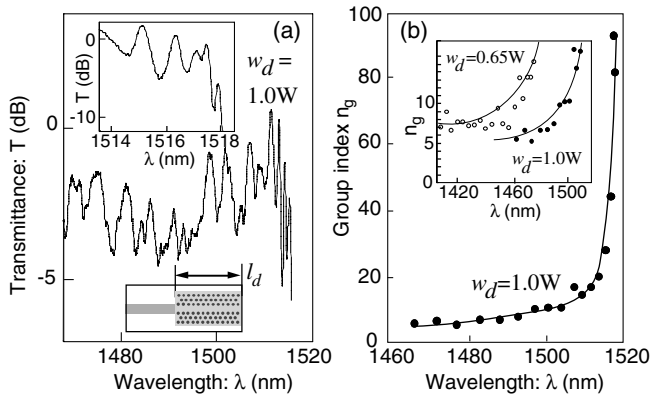


FIG. 4. (a) Transmission spectrum of a $w_d = 1.0$ W sample ($l_d = 88a$), showing clear Fabry-Perot oscillation. The inset is a magnified plot. Schematic of FP cavities with the length of l_d is also shown. (b) Deduced group index n_g vs wavelength for $w_d = 1.0$ W and $w_d = 0.65$ W.

Fig. 2. The solid and open circles are the cutoffs due to the mode gap and the light line, respectively. The experimentally observed transmission windows for different w_d are explained very well by theoretical calculation, which directly proves that these theoretically predicted waveguiding modes are actually realized in our LDWGs. To further examine the nature of the cutoffs, we measured a shorter 1.0 W sample ($l_d = 88a$). The measured transmission spectrum [Fig. 2(j)] shows that the higher-frequency cutoff becomes less significant and almost invisible, although the lower-frequency cutoff remains the same as that for $l_d = 441a$. Since quasiwaveguiding modes with a propagation loss of the order of 100 dB/mm can transmit through 34- μ m-long LDWGs with only a few dB loss, this result can be understood from the above interpretation. This implies that we have to take these quasiwaveguiding modes into account if we wish to have a strictly single-mode waveguide. Our calculation confirmed that this condition is satisfied for $w_d < 0.80$ W.

Our results make the LDWG waveguiding characteristics fairly clear, but they do not tell about the dispersion characteristics. In the theoretical curves (Fig. 3), we can see that the dispersion is very unusual but such a property has not been proven. This is because the transmission window yields only information on the frequency regime, whereas we have to obtain information on the wavevector regime to determine the dispersion. Since one of the most distinctive features of LDWGs is their unique disappearing characteristic, we next proceeded to examine the dispersion.

It is possible to utilize interference phenomena to obtain information on wavevector k . In our case, the easiest way to do this was to detect Fabry-Perot (FP) interference inside the sample itself. Since our sample intrinsically has two mirrors (a cleaved facet of the LDWG and the boundary between the LDWG and ridge waveguide) which form

a FP cavity, as shown in Fig. 4(a). FP resonance oscillation can be already seen in some of the spectra in Fig. 2. Figure 4(a) is the spectrum of a 1.0 W sample obtained with higher resolution, showing apparent FP-type oscillation with a 2–5 dB amplitude. Note that the oscillation period is not constant and becomes smaller as λ becomes longer, suggesting a strongly dispersive character. Since the k spacing of the FP oscillation should be $\Delta k = a/2l_d$, which leads to a group velocity of $v_g = c/n_g$ where n_g is the group index $n_g = \lambda^2/(2lc\Delta\lambda)$, the decrease in the oscillation period implies a decrease (increase) in group velocity (n_g). The inset in the figure is a magnified spectrum showing that clear oscillating behavior remains even when the period becomes very small. We deduced n_g from the measured oscillation using the above relation. Figure 4(b) summarizes the deduced n_g for two types of samples as a function of λ . We confirmed that samples with the same w_d but different l_d (from $88a$ to $441a$) produce the same n_g . The dispersion of n_g seen in Fig. 4(b) is extremely large compared to that of conventional waveguides and photonic crystal fibers [10,13]. In the case for $w_d = 1.0$ W, the deduced n_g varies approximately from 5 to 90. This means that the speed of light propagation along the LDWG is 5 to 90 times slower than that in air. This result demonstrates that waveguiding modes with very large group dispersion and extremely slow velocity are realized in LDWGs.

The effect of optical processes induced by light-matter interaction such as amplification or wavelength conversion will be increased if the group velocity inside the media becomes slow. In other words, effective light-matter interaction is enhanced as n_g becomes large. For conventional waveguides, n_g is comparable to the refractive index of the component materials. The observed large reduction in group velocity with 2 order of magnitude indicates that various kinds of optical processes will be enhanced for this LDWG. A recent report on light-atom coupled systems has shown that light velocity can be greatly reduced by using laser cooling [14]. Although the basic physics is different, our result demonstrates another way of controlled braking light propagation.

Figure 4(b) shows that the enhancement of n_g is largest near the mode gap where the anticrossing effect is dominant. However, n_g is still larger than the material phase index n_p (3.46 for Si) even when λ is far from the mode gap. This feature is more pronounced for narrower LDWGs. The inset in Fig. 4(b) shows n_g for a 0.65W sample is around 7–8 in this region, which is more than twice as large as the material index. Generally, n_g is expressed as $n_g = n_p - \lambda(dn_p/d\lambda)$, and therefore $n_g < n_p$ if the structure has *anomalous* dispersion ($dn/d\lambda > 0$) which is mostly the case for conventional waveguides (here, we ignore the material dispersion). But waveguides with large Δn can have *normal* dispersion ($dn/d\lambda < 0$) and thus $n_g > n_p$. The increase of n_g is the result of the wave function being squeezed within the

waveguides, and thus it is more pronounced for larger Δn . However, even for the Si-air stripe waveguides (nearly the largest Δn), n_g cannot be as large as 5. This is the limitation of total-internal reflection confinement, which does not apply for LDWGs because the confinement mechanism is fundamentally different. These results show that we can design various types and strengths of dispersion in LDWGs that can be fabricated by the current technology.

Finally, we use the experimentally determined n_g value to construct the full dispersion curve, which is possible by integrating n_g [15]. We plot the deduced dispersion for 1.0 and 0.65 W in Fig. 3. For both samples, the experimentally determined dispersion curvature is fairly close to the calculated one. Note that the agreement is achieved even where the curve heavily deviates from linear. This agreement demonstrates that theoretical designing of waveguiding modes is realistically possible by using the current nanofabrication technology.

We think that the slowest value of group velocity is still limited by technological reasons (e.g., structural imperfection), but there is something still worthwhile to examine further. In our case, the very large enhancement is realized for $w_d < 1.0$ W, and we did not observe the region of $n_g > 20$ for narrower LDWGs ($w_d < 0.80$ W) although the propagation loss is comparable. We regard the inclusion of GG modes as effective to realize very small velocity mode (note that LDWG modes for the $w_d = 1.0$ W mode are strongly mixed with GG modes near the cutoff, but those for $w_d < 0.80$ W are not).

The highly dispersive nature, which has been directly demonstrated in this work, is one of the most distinctive features for LDWGs, and this strong dispersion will open up new possibilities for functional waveguides. Combinations of the unusual dispersion with various optical nonlinearity phenomena are very interesting because high photon density can be easily realized in these waveguides due to the strong confinement within the nanoscale cross section. The achieved agreement between experiment and theory suggests that we can design various unique dispersions by controlling the geometrical configuration of PCs. By using this technology, we can control the light transmission

through a light path in a PC platform with a great degree of freedom.

We thank T. Tamamura, H. Morita, S. Ishihara, H. Takayanagi, M. Morita, and T. Mukai for their support.

-
- [1] E. Yablonovitch, Phys. Rev. Lett. **58**, 2059 (1987).
 - [2] T.F. Krauss, R.M. De La Rue, and S. Brand, Nature (London) **383**, 699 (1996).
 - [3] J.D. Joannopoulos, P.R. Villeneuve, and S. Fan, Nature (London) **386**, 143 (1997).
 - [4] A. Mekis, J.C. Chen, I. Kurland, S. Fan, P.R. Villeneuve, and J.D. Joannopoulos, Phys. Rev. Lett. **77**, 3787 (1996).
 - [5] E. Chow, S.Y. Lin, S.G. Johnson, P.R. Villeneuve, J.D. Joannopoulos, J.R. Wendt, G.A. Vawter, W. Zubrzycki, H. Hou, and A. Alleman, Nature (London) **407**, 983 (2000).
 - [6] N. Kawai, K. Inoue, N. Carlsson, N. Ikeda, Y. Sugimoto, K. Asakawa, and T. Takemori, Phys. Rev. Lett. **86**, 2289 (2001).
 - [7] M. Loncar, D. Nedeljkovic, T. Doll, J. Vuckovic, A. Scherer, and T.P. Pearsall, Appl. Phys. Lett. **77**, 1937 (2000).
 - [8] T. Baba, N. Fukaya, and J. Yonekura, Electron. Lett. **35**, 654 (1999).
 - [9] S. Y. Lin, E. Chow, S. G. Johnson, and J. D. Joannopoulos, Opt. Lett. **25**, 1297 (2000).
 - [10] M.J. Gander, R. McBride, J.D.C. Jones, D. Mogilevtsev, T. A. Birks, J. C. Knight, and P. St. J. Russel, Electron. Lett. **35**, 63 (1999); R.F. Cregan, B.J. Mangan, J.C. Knight, T. A. Birks, P. St. J. Russel, P.J. Roberts, and D. C. Allan, Science **285**, 1537 (1999).
 - [11] C. Takahashi, J. Takahashi, M. Notomi, and I. Yokohama, in *Microphotonics: Materials, Physics and Applications*, MRS Symposia Proceedings No. 637 (Materials Research Society, Pettsbyrgg, 2001).
 - [12] A. Chutinan and S. Noda, Phys. Rev. B **62**, 4488 (2000).
 - [13] Small group velocity was also observed in bulk 1D photonic crystals without defects [V.N. Astratov *et al.*, Appl. Phys. Lett. **77**, 178 (2000)].
 - [14] L.V. Hau, S.E. Harris, Z. Dutton, and C.H. Behroozi, Nature (London) **397**, 594 (1999).
 - [15] This determination has uncertainty in the position of the k -axis origin due to the uncertainty of integration constants.